

## Minimal volume photoacoustic cell measurement of thermal diffusivity: Effect of the thermoelastic sample bending

L. F. Perondi and L. C. M. Miranda

Citation: *J. Appl. Phys.* **62**, 2955 (1987); doi: 10.1063/1.339380

View online: <http://dx.doi.org/10.1063/1.339380>

View Table of Contents: <http://jap.aip.org/resource/1/JAPIAU/v62/i7>

Published by the [American Institute of Physics](#).

---

### Additional information on J. Appl. Phys.

Journal Homepage: <http://jap.aip.org/>

Journal Information: [http://jap.aip.org/about/about\\_the\\_journal](http://jap.aip.org/about/about_the_journal)

Top downloads: [http://jap.aip.org/features/most\\_downloaded](http://jap.aip.org/features/most_downloaded)

Information for Authors: <http://jap.aip.org/authors>

## ADVERTISEMENT

The advertisement banner for AIP Advances features a green and yellow wavy background. On the left, the text 'Explore AIP's open access journal:' is written in blue. To its right, a list of three bullet points in blue text describes the journal's features: 'Rapid publication', 'Article-level metrics', and 'Post-publication rating and commenting'. In the center, the 'AIP Advances' logo is displayed, with 'AIP' in blue and 'Advances' in green, accompanied by a series of orange dots. On the right side, a circular seal with a green border contains the text 'Now Indexed in Thomson Reuters Databases' in black.

**AIP Advances**

Now Indexed in  
Thomson Reuters  
Databases

**Explore AIP's open access journal:**

- Rapid publication
- Article-level metrics
- Post-publication rating and commenting

# Minimal-volume photoacoustic cell measurement of thermal diffusivity: Effect of the thermoelastic sample bending

L. F. Perondi and L. C. M. Miranda

*Ministério da Ciência e Tecnologia, Instituto de Pesquisas Espaciais, Laboratório Associado de Sensores e Materiais, Caixa Postal 515, 12201 São José dos Campos, SP, Brazil*

(Received 17 November 1986; accepted for publication 19 May 1987)

A minimal-volume photoacoustic cell method is demonstrated for obtaining the thermal diffusivity of solids. It is based on the measurement of the acoustic signal as a function of the modulation frequency in the region where the sample is thermally thick. The method is tested by using metal, semiconductor, and polymer samples.

## INTRODUCTION

Since the revival of the photoacoustic (PA) spectroscopy in the early seventies, a variety of photothermal techniques have been proposed to detect the temperature oscillation due to a periodic irradiation of a sample. In particular, one of these techniques, named optothermal or open photoacoustic cell (OPC) technique,<sup>1</sup> consists in measuring the expansion of a thin solid plate (usually a sapphire plate) in thermal contact with the sample. This technique has been successfully applied to study the optical spectra of liquids (e.g., dilute solution of nigrosine)<sup>1</sup>, sedimentation of whole blood,<sup>2</sup> and the discrimination of bulk and surface optical absorption coefficients.<sup>3</sup> The theory for the open-cell photoacoustic signal was described by Helander in Refs. 4 and 5. A modified version for the open photoacoustic cell was proposed by McQueen.<sup>6</sup> It consisted of a sapphire disk mounted onto a ring-shaped piezoelectric crystal. The absorbing sample is placed on the sapphire window. When light is sent through the window and becomes partly absorbed by the sample, which is in thermal contact with the window, radial expansion gives rise to an electric signal from the piezoelectric crystal. This open-cell sensor is shown in Fig. 1(a). The wavelength of the incident light can either be swept in order to record an absorption spectrum or kept fixed for specific quantitative measurements of a particular substance.

In this paper we propose a microphone detection version for the OPC technique and apply it to the problem of thermal characterization of solid samples. The schematic cross section of the proposed OPC configuration is shown in Fig. 1(b). It consists of mounting the sample directly onto a circular electret microphone. It is an open-cell detection configuration in the sense that the sample is placed on top of the detection system itself, as in the case of piezoelectric and pyroelectric detections. The typical design<sup>7,8</sup> of the electret microphone consists of a metallized electret diaphragm (12- $\mu\text{m}$  Teflon with a 500–1000-Å-thick deposited metal electrode) and a metal backplate separated from the diaphragm by an air gap (45  $\mu\text{m}$ ). The metal layer and the backplate are connected through a resistor  $R$ . The front sound inlet is a circular hole of 2 mm diam, and the front air chamber adjacent to the metallized face of the diaphragm is roughly 1 mm long. As a result of the periodic heating of the sample by the absorption of modulated light, the pressure in the front chamber oscillates at the chopping frequency, causing dia-

phragm deflections, generating a voltage  $V$  across the resistor  $R$ . That is, the proposed technique consists of using the front chamber of the microphone itself as the usual gas chamber of conventional photoacoustics and may be called a minimal-volume photoacoustic detection. Its advantages over conventional spectroscopy are the use of a reduced gas chamber, with no further transducer medium needed as in conventional spectroscopy and minimal requirements of experimental arrangement and cell machining. The use of a minimal gas chamber considerably increases the signal-to-noise ratio.

## THEORY

Applying the simple one-dimensional thermal diffusion model of Rosencwain and Gersho<sup>9</sup> to the arrangement schematically shown in Fig. 2(a) one gets for the pressure fluctuation  $p_{\text{th}}$  in the air chamber

$$p_{\text{th}} = \frac{\gamma P_0 I_0 (\alpha_g \alpha_s)^{1/2}}{2\pi l_g T_0 k_s f} \frac{e^{j(\omega t - \pi/2)}}{\sinh(l_s \sigma_s)}, \quad (1)$$

where  $\gamma$  is the air specific heat ratio,  $P_0$  ( $T_0$ ) is the ambient pressure (temperature),  $I_0$  is the absorbed light intensity,  $f$  is the modulation frequency, and  $l_i$ ,  $k_i$ , and  $\alpha_i$  are the length, thermal conductivity, and thermal diffusivity of material  $i$ , respectively. Here the subscript  $i$  denotes the sample ( $s$ ) and gas ( $g$ ) media, respectively, and  $\sigma_i = (1+j)\alpha_i$ ,  $\alpha_i = (\pi f / \alpha_i)^{1/2}$ , is the complex thermal diffusion coefficient of material  $i$ . In arriving at Eq. (1) we have assumed that the sample is optically opaque to the incident light and that the heat flux into the surrounding air is negligible. The optical opaqueness condition means that all the light is absorbed at the sample surface at  $z = -l_s/2$  [cf. Fig. 2(a)] and is a reasonable assumption for metals and most semiconductors irradiated by visible light.

For a thermally thin sample (i.e.,  $l_s \alpha_s \ll 1$ ), Eq. (1) reduces to

$$p_{\text{th}} \approx \frac{\gamma P_0 I_0 \alpha_g^{1/2} \alpha_s}{(2\pi)^{3/2} T_0 l_g l_s k_s} \frac{e^{j(\omega t - 3\pi/4)}}{f^{3/2}}. \quad (2)$$

That is, the amplitude of the PA signal decreases as  $f^{-1.5}$  as one increases the modulation frequency. In contrast, at high modulation frequencies, such that the sample is thermally

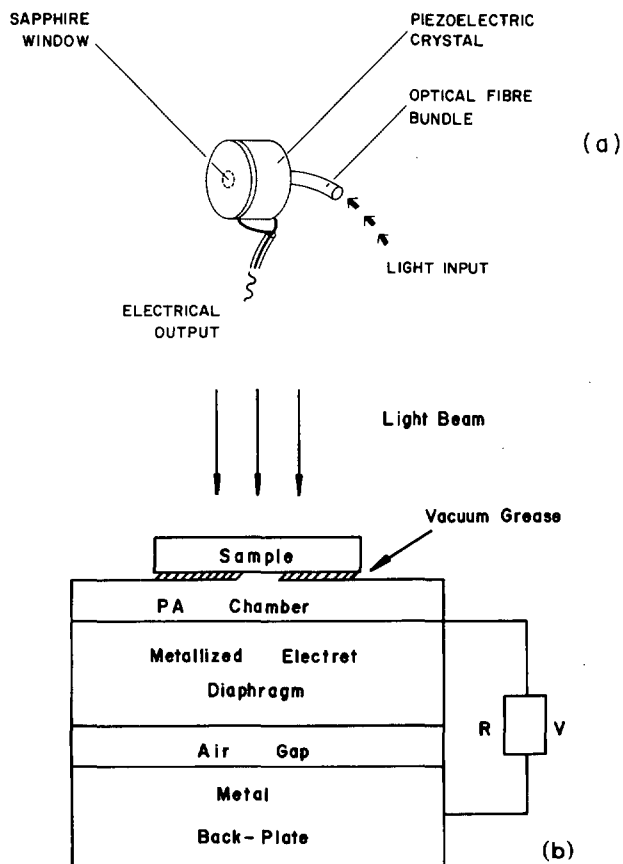


FIG. 1. (a) Schematic ring-shaped open photoacoustic cell and (b) proposed open photoacoustic cell with the use of the front air chamber of a common electret microphone as the transducer medium.

thick (i.e.,  $l_s a_s \gg 1$ ), one gets

$$p_{th} \sim \frac{\gamma P_0 I_0 (\alpha_g \alpha_s)^{1/2}}{\Pi T_0 l_g k_s} \frac{e^{-l_s \sqrt{\pi f / \alpha_s}}}{f} \times e^{j(\omega t - \pi/2 - l_s a_s)}. \quad (3)$$

Equation (3) means that, for a thermally thick sample, the amplitude of the PA signal decreases exponentially with the modulation frequency as  $(1/f) \exp(-a\sqrt{f})$ , where  $a = l_s \sqrt{\pi / \alpha_s}$ , whereas its phase  $\phi_{th}$  decreases linearly with  $\sqrt{f}$ , namely,  $\phi_{th} = -\pi/2 - a\sqrt{f}$ . The thermal diffusivity  $\alpha_s$  can then be obtained from the high-modulation-frequency behavior of either the signal amplitude or its phase. In the case of the signal amplitude,  $\alpha_s$  is obtained from the experimental data fitting from the coefficient  $a$  in the argument of the exponential  $(-a\sqrt{f})$ , whereas when using the signal phase data,  $\alpha_s$  is obtained from the phase slope as a function of  $\sqrt{f}$ .

However, in the case of plate-shaped solid samples surrounded by air, the contribution of the PA signal from the thermoelastic bending of the sample cannot be neglected, especially in the case of thermally thick samples, as has been demonstrated by Rousset *et al.*<sup>10</sup> in both photothermal deflection and conventional PA experiments. This effect is essentially due to the temperature gradient inside the sample along the  $z$  axis and is schematically depicted in Fig. 2(b).

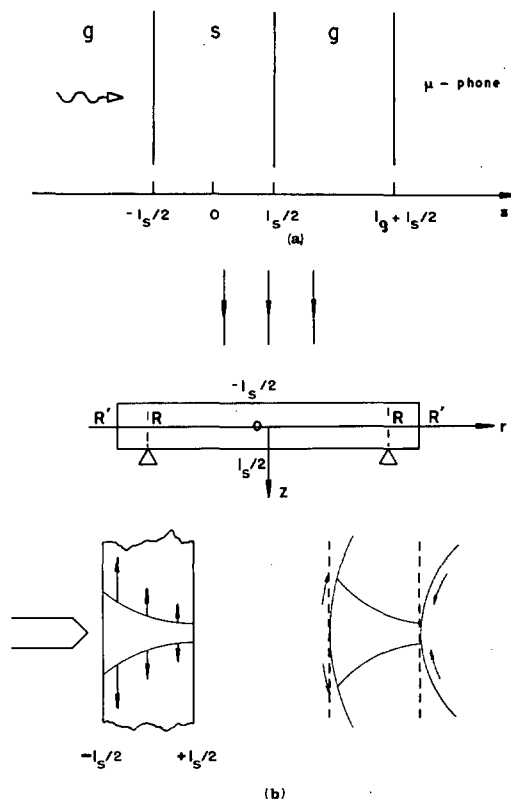


FIG. 2. (a) Schematic open photoacoustic cell geometry and (b) geometry and sources of surface strain for the thermoelastic bending.  $R'$  and  $R$  are the sample and the microphone inlet hole radius, respectively.

Because of the existence of this temperature gradient parallel to the  $z$  axis, thermal expansion depends on  $z$ . This  $z$  dependence of the displacement along the radial direction induces a bending of the plate in the  $z$  direction (drum effect). That is, the vibrating sample acts as a mechanical piston, thereby contributing to the PA signal. The contribution from the sample bending is formally described by the coupled set of thermoelastic equations, similarly to the case of the piezoelectric PA detection.<sup>11</sup> The following assumptions are made. We neglect the heating caused by the sample displacement (elastic waves). Taking into account the heating due to the elastic waves in the thermal diffusion equation is equivalent<sup>12</sup> to multiplying the term  $\partial T / \partial t$  by  $[1 + (C_p - C_v) / C_p]$ , where  $C_p$  and  $C_v$  are the heat capacities per unit volume. Recalling that  $C_p - C_v = T_0 B (3\alpha_T)^2$ , where  $B$  is the bulk modulus, and  $\alpha_T$  is the linear thermal expansion coefficient, it can be shown that, for most solids,  $C_p - C_v / C_p \sim 10^{-3}$ . This means that the temperature distribution  $T_s$  in the sample is given by the classical thermal diffusion equation without the displacement terms. For the configuration shown in Fig. 2(a), and assuming that all light is absorbed at the surface, one gets<sup>10</sup>

$$T_s(z) = \frac{I_0}{k_s \sigma_s} \frac{\cosh\{[z - (l_s/2)] \sigma_s\}}{\sinh(l_s \sigma_s)} e^{j\omega t}. \quad (4)$$

We also neglect in the displacement equation the inertial term since the experiments are done at low frequencies. The inertial term is negligible when  $\omega R' \ll v_s$ , where  $R'$  is the sample radius, and  $v_s = [(E / (1 - \nu^2)) \rho]^{1/2}$  is the sound ve-

locity. Here  $E$  is the Young modulus, and  $\nu$  is the Poisson ratio. Since for most solids,  $v_s \sim 10^5$  cm/s, this condition is well satisfied for frequencies below 10 kHz in a 1-cm-wide sample. Finally, we assume that the sample is cylindrically symmetric and thin enough such that  $l_s \ll R'$ . In this case the plane stress condition is applicable; i.e., one has  $\sigma_{zz} = \sigma_{rz} = 0$  along the  $z$  direction, where  $\sigma_{ij}$  is the stress tensor.

Under these circumstances, solving the set of thermoelastic equations for the sample displacement  $u_r$  and  $u_z$  along the radial and  $z$  directions subjected to the boundary conditions that the sample is simply supported at  $r = R$  and  $z = l_s/2$  and that at the edges  $r = R'$  it is free of forces and moments, one gets<sup>10</sup>

$$u_z(r, z) = \alpha_T \left\{ \frac{6(R^2 - r^2)}{l_s^3} M_T + \frac{1 + \nu}{1 - \nu} \int_{l_s/2}^z dz T_s - \frac{\nu}{1 - \nu} \times \left[ \frac{12M_T}{l_s^3} \left( z^2 - \frac{l_s^2}{4} \right) + \frac{2N_T}{l_s} \left( z - \frac{l_s}{2} \right) \right] \right\} \quad (5)$$

with

$$M_T = \int_{-l_s/2}^{l_s/2} dz z T_s, \quad N_T = \int_{-l_s/2}^{l_s/2} dz T_s. \quad (6)$$

The first term in Eq. (5) represents the bending of the sample, and the other ones are due to the thickness dilatation.

Knowing the sample displacement along the  $z$  direction, one can calculate the thermoelastic contribution  $p_{el}$  to the pressure fluctuation in the PA chamber using the vibrating sample piston model of McDonald and Wetzel<sup>13</sup> as  $p_{el} = \gamma P_0 \Delta V / V_0$ . Here  $\Delta V$  is the volume change due to the sample surface displacement. One has

$$p_{el} = \frac{\gamma P_0 2\pi}{V_0} \int_0^R dr r u_z \left( r, \frac{l_s}{2} \right). \quad (7)$$

Using Eqs. (4), (5), and (6) in Eq. (7), one finally obtains

$$p_{el} = \frac{3\alpha_T R^4}{R_c^2 l_s^2} \times \frac{\gamma P_0 I_0}{l_g K_s \sigma_s^2} \left( \frac{\cosh(l_s \sigma_s) - (l_s \sigma_s / 2) \sinh(l_s \sigma_s) - 1}{l_s \sigma_s \sinh(l_s \sigma_s)} \right) e^{j\omega t}, \quad (8)$$

where  $R_c$  is the radius of the PA chamber in front of the diaphragm. It follows from Eq. (8) that for a thermally thin sample ( $l_s \sigma_s \ll 1$ ), the thermoelastic contribution to the PA signal reduces to

$$p_{el} \approx \frac{\alpha_T R^4 \gamma P_0 I_0}{8 R_c^2 l_g k_s} e^{j(\omega t + \pi)}. \quad (9)$$

That is, the PA signal becomes independent of the modulation frequency while its phase  $\phi_{el}$  approaches  $180^\circ$ . In contrast, for a thermally thick sample one has

$$p_{el} \approx \frac{3\alpha_T R^4 \gamma P_0 I_0 \alpha_s}{4\pi R_c^2 l_s^2 l_g k_s f} \left[ \left( 1 - \frac{1}{x} \right)^2 + \frac{1}{x^2} \right]^{1/2} e^{j[\omega t + (\pi/2) + \phi]} \quad (10)$$

where  $x = l_s \alpha_s = l_s (\pi f / \alpha_s)^{1/2}$ , and

$$\tan \phi = 1/(x - 1). \quad (11)$$

Equations (10) and (11) mean that the thermoelastic contribution, at high modulation frequencies such that  $x \gg 1$ , varies as  $f^{-1}$ , and its phase  $\phi_{el}$  approaches  $90^\circ$  as

$$\phi_{el} \approx \pi/2 + \arctan [1/(x - 1)]. \quad (12)$$

Thus, for a thermally thick sample, if the thermoelastic contribution is dominant, the thermal diffusivity can be evaluated from the modulation frequency dependence of either the signal amplitude [Eq. (10)] or its phase [Eq. (12)].

## RESULTS AND DISCUSSION

The experimental setup for the measurement of thermal diffusivity consisted of a 400 W Xe lamp whose polychromatic beam is mechanically chopped and uniformly focused into the sample. The sample is placed on top of the condenser microphone as shown in Fig. 1(b). A lock-in amplifier is used to analyze the amplitude and phase of the microphone signal. The samples studied were disks of Al ( $l_s = 500 \mu\text{m}$ ,  $R' = 2.0$  mm), *p*-type Si ( $l_s = 350 \mu\text{m}$ ,  $R' = 2.0$  mm), low-density polyethylene (LDPE) ( $l_s = 240 \mu\text{m}$ ,  $R' = 2.5$  mm), high-density polyethylene (HDPE) ( $l_s = 105 \mu\text{m}$ ,  $R' = 2.5$  mm), and polypropylene ( $l_s = 195 \mu\text{m}$ ,  $R' = 2.5$  mm). In the case of the transparent polymer samples, the condition of optical opaqueness, implicit in the theory described above, was achieved by coating the absorbing surface of the sample with a  $1 \mu\text{m}$ -thick Cr film.

In Fig. 3 we show the dependence of the PA signal on the modulation frequency for the Al sample. For frequencies up to roughly 130 Hz, the signal exhibits a frequency dependence close to  $f^{-1.5}$ . This is the typical frequency dependence one would expect from the thermal diffusion model for a thermally thin sample [cf. Eq. (2)]. In fact, for a  $500\text{-}\mu\text{m}$ -thick Al sample, the characteristic frequency  $f_c (= \alpha_s / \pi l_s^2)$  for the transition between the thermally thin and thick regime, obtained from the condition  $l_s \alpha_s = 1$ , is  $f_c = 120$  Hz. In the thermally thick region, namely, for  $f \gg f_c$ , the PA signal exhibited a roughly  $f^{-1.0}$  frequency dependence, instead of the exponential behavior [cf. Eq. (3)]

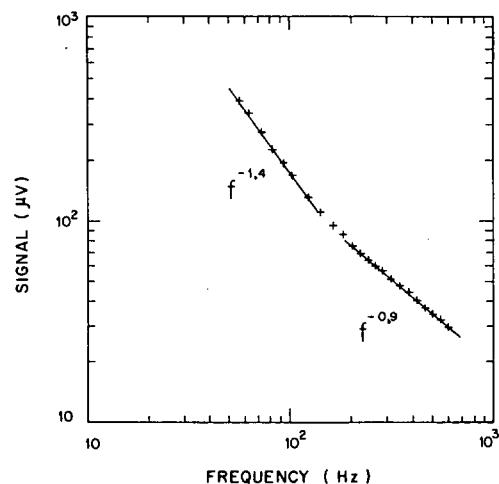


FIG. 3. Microphone output voltage as a function of the chopping frequency for the  $500\text{-}\mu\text{m}$ -thick Al sample. For frequencies greater than 130 Hz the signal behaves roughly as  $f^{-1.0}$ .

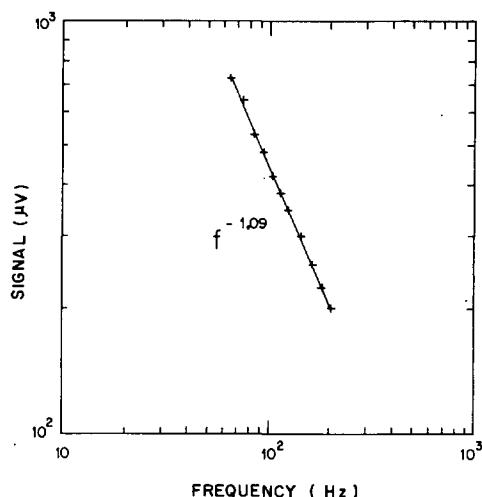


FIG. 4. Microphone output voltage as a function of the chopping frequency for the 240- $\mu\text{m}$ -thick LDPE sample. The frequency dependence was always a  $f^{-1.0}$  in the whole range of our measurements.

predicted by the thermal diffusion model. The  $f^{-1.0}$  frequency dependence of the PA signal of a thermally thick sample suggests [cf. Eq. (10)] that in this frequency range the thermoelastic bending is the dominant mechanism responsible for the acoustic signal. Except for the Si sample, in all other samples studied the thermoelastic bending was always dominant in the thermally thick region. This was manifested by the  $f^{-1}$  frequency behavior of the acoustic signal amplitude, for  $f \gg f_c$ , and the fact that the phases of the measured signals were frequency dependent. In fact, only the  $f^{-1}$  frequency dependence of the signal amplitude, in the thermally thick region, does not assure us that the thermoelastic bending is the dominant mechanism. As shown in Ref. 10, the thermal dilatation also leads to the same  $f^{-1}$  frequency dependence for the signal amplitude. However, the thermal dilatation mechanism produces<sup>10</sup> a signal whose phase is independent of the modulation frequency and equal to  $-90^\circ$ , a fact that was never observed in our experiments. We are thus led to the conclusion that the thermoelastic bending is indeed the dominant mechanism. In Fig. 4 we show the observed signal frequency dependence for a typical polymer sample, namely, the LDPE sample. For this sample the existing literature value of  $\alpha_s$  ( $= 0.0016 \text{ cm}^2/\text{s}$ ) yields  $f_c = 0.9 \text{ Hz}$ . This

TABLE I. Comparison of the thermal diffusivity values obtained from the OPC technique with the values quoted in the literature.

Material	Measured ( $\text{cm}^2/\text{s}$ )	Literature values ( $\text{cm}^2/\text{s}$ )
Aluminum	0.99	0.94 <sup>a</sup>
Silicon	0.87	0.85 <sup>a</sup>
Low-density polyethylene	0.0017	0.0016 <sup>b</sup>
High-density polyethylene	0.0020	0.0022 <sup>b</sup>
Polypropylene	0.0011	0.0009 <sup>b</sup>

<sup>a</sup> Reference 14.

<sup>b</sup> Reference 15.

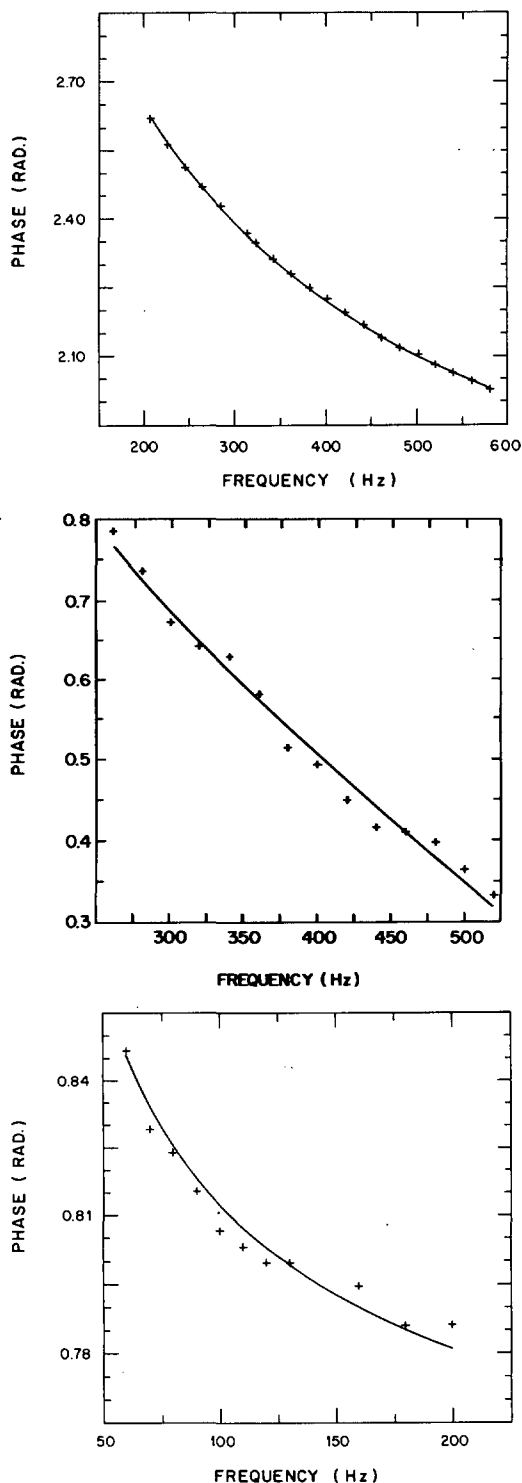


FIG. 5. PA signal phase dependence on the chopping frequency for the (a) Al, (b) Si, and (c) LDPE samples. The solid curves are the theoretical curves for the phase dependence as a function of the modulation frequency as given by the thermoelastic bending and the thermal diffusion models with the use of the results of the data fitting.

means that in the frequency range of our measurements, 50–600 Hz, the sample is thermally thick. The observed frequency dependence ( $\sim f^{-1.0}$ ) points again at the thermoelastic bending as the dominant mechanism responsible for the PA signal. The only sample that exhibited the exponential decay

as a function of  $\sqrt{f}$  was the Si, which entails that, for this sample, thermal diffusion is the dominant mechanism. This is physically understood by the fact that, of the samples studied, Si has the smallest thermal expansion coefficient ( $\sim 1.5 \times 10^{-6} \text{ }^\circ\text{C}^{-1}$ ) as compared with Al ( $\sim 24 \times 10^{-6} \text{ }^\circ\text{C}^{-1}$ ) and the polymer samples ( $\sim 10^{-4} \text{ }^\circ\text{C}^{-1}$ ).

The thermal diffusivity was obtained from the fitting of the PA phase data, in the thermally thick region, to the corresponding theoretical expressions. In the case of the Al and the polymer samples the PA phase data was fitted to the predicted phase behavior due to the thermoelastic contribution given by Eq. (12). For the Si sample, which was always described by the thermal diffusion model, the phase data was fitted to  $\phi_{\text{th}} = -\pi/2 - a\sqrt{f}$ , where  $a = l_s(\pi/\alpha_s)^{1/2}$ . In Table I we summarize the results we have obtained for the thermal diffusivity and compare them with the literature values. In Figure 5 we show the phase data of our Al, Si, and LDPE samples as a function of the modulation frequency. The solid curves in this plot correspond to the theoretical expressions for the thermoelastic bending and thermal diffusion contributions with the use of the results of our data fitting. The good agreement between the observed values of the thermal diffusivity and the literature values shows that the proposed minimal-volume method is a simple and accurate technique for obtaining the thermal diffusivity. Its ad-

vantages over the conventional photoacoustic techniques for the thermal diffusivity measurements<sup>16-19</sup> are the use of a minimal gas chamber and, consequently, an increased signal-to-noise ratio, and its adaptability to practical restrictions imposed by experimental system requirements, especially when minimal preparation is required.

- <sup>1</sup>P. Helander, J. Photoacoust. **1**, 103 (1982).
- <sup>2</sup>P. Helander, J. Photoacoust. **1**, 203 (1982).
- <sup>3</sup>P. Helander and I. Lundström, J. Appl. Phys. **54**, 5069 (1983).
- <sup>4</sup>P. Helander, J. Photoacoust. **1**, 251 (1982).
- <sup>5</sup>J. Helander, J. Appl. Phys. **59**, 3339 (1986).
- <sup>6</sup>D. H. McQueen, J. Phys. E **16**, 738 (1983).
- <sup>7</sup>G. M. Sessler, J. Acoust. Soc. Am. **35**, 1354 (1963).
- <sup>8</sup>G. M. Sessler and J. E. West, J. Acoust. Soc. Am. **53**, 1589 (1973).
- <sup>9</sup>A. Rosencwaig and Gersho, J. Appl. Phys. **47**, 64 (1976).
- <sup>10</sup>G. Rousset, F. Lepoutre, and L. Bertrand, J. Appl. Phys. **54**, 2383 (1983).
- <sup>11</sup>W. Jackson and N. M. Amer, J. Appl. Phys. **51**, 3343 (1980).
- <sup>12</sup>W. Nowacki, *Thermoelasticity* (Pergamon, Oxford, 1962).
- <sup>13</sup>F. A. McDonald and G. C. Wetzel, Jr., J. Appl. Phys. **49**, 2313 (1978).
- <sup>14</sup>L. R. Touloukian, R. W. Powell, C. Y. Ho, and M. C. Nicolasu, *Thermal Diffusivity* (IFI/Plenum, New York, 1973).
- <sup>15</sup>D. Grzegorzczak and G. Feineman, *Handbook of Plastics and Electronic* (Reston, Reston, VA, 1974).
- <sup>16</sup>M. J. Adams and G. F. Kirkbright, Analyst **102**, 281 (1977).
- <sup>17</sup>Z. Yasa and N. Amer, in Topical Meeting on Photoacoustic Spectroscopy, Ames, 1979 (unpublished), paper WA5-1.
- <sup>18</sup>P. Charpentier, F. Lepoutre, and L. Bertrand, J. Appl. Phys. **53**, 608 (1982).
- <sup>19</sup>O. Pessoa Jr., C. L. Cesar, N. A. Patel, H. Vargas, C. C. Ghizoni, and L. C. M. Miranda, J. Appl. Phys. **59**, 1316 (1986).